Original Article

Modelling tissue specific RBE for different radiation qualities based on a multiscale characterization of energy deposition

Erik Almhagen [a,b,1,*], Fernanda Villegas [c], Nina Tilly [a,d], Lars Glimelius [e], Erik Traneus [e], Anders Ahnesjö [a]

[a] Medical Radiation Sciences, Department of Immunology, Genetics and Pathology, Uppsala University, Akademiska Sjukhuset, SE-75185 Uppsala; [b] The Skandion Clinic, Uppsala; [c] Radiotherapy Physics and Engineering, Medical Radiation Physics and Nuclear Medicine, Karolinska University Hospital, SE-17176 Stockholm; [d] Elekta Instrument AB, Box 7593, Stockholm SE-10393; and [e] RaySearch Laboratories, Stockholm, Sweden

ABSTRACT

Purpose: We present the nanoCluE model, which uses nano- and microdosimetric quantities to model RBE for protons and carbon ions. Under the hypothesis that nano- and microdosimetric quantities correlates with the generation of complex DNA double strand breaks, we wish to investigate whether an improved accuracy in predicting LQ parameters may be achieved, compared to some of the published RBE models.
Methods: The model is based on experimental LQ data for protons and carbon ions. We generated a database of track structure data for a number of proton and carbon ion kinetic energies with the Geant4-DNA Monte Carlo code. These data were used to obtain both a nanodosimetric quantity and a set of microdosimetric quantities. The latter were tested with different parameterizations versus experimental LQ-data to select the variable and parametrization that yielded the best fit.
Results: For protons, the nanoCluE model yielded, for the ratio of the linear LQ term versus the test data, a root mean square error (RMSE) of 1.57 compared to 1.31 and 1.30 for two earlier other published proton models. For carbon ions the RMSE was 2.26 compared to 3.24 and 5.24 for earlier published carbon ion models.
Conclusion: These results demonstrate the feasibility of the nanoCluE RBE model for carbon ions and protons. The increased accuracy for carbon ions as compared to two other considered models warrants further investigation.

Since the mechanisms of radiation response are acting over several orders of resolution a multiscale approach is inevitable when trying to model the variation in response between radiation qualities with the RBE (Relative Biological Efficiency) factor. The current clinical practice for protons is to apply a constant factor of 1.1 [1] while for carbon ions the larger RBE variations have necessitated the use of models such as e.g. the LEM (Local Effect Model) [2], the MKM (Microdosimetric Kinetic Model) [3] or the mMKM (modified Microdosimetric Kinetic Model) [4]. A fully mechanistic model is however, given the complexity of interacting systems in living matter, an overwhelming task which has not yet been demonstrated.

In this work we present an empirical RBE model based on radiation characteristics including the clustering of particle interactions at the nanometric or DNA scale, characteristic target sizes at the length scale of cell nuclei derived from microdosimetry data, and the α/β ratio for photons, the latter as a proxy for higher level responses at the scale of tumors and tissues. We have investigated routes to an optimal parameterization of multiscale variables for predicting RBE based on available cell survival assay linear-quadratic (LQ) data for protons and carbon ions. We name our framework nanoCluE (nanometric Cluster Effect) after the nanodosimetric part that stems from a previous study [5] that explored the correlation of RBE for V79 cell line to the clustering of energy deposition (ED) events at the nanometric scale of the lower levels of the DNA winding packaging. Since cell nuclei contains DNA void domains to effectively constitute cavities for which the microdosimetric spread of overall energy deposition will be of importance [6,7], we include a microdosimetric dependence based on earlier work for characteristic size determination [8]. We introduce some particle specific parameterizations of intermediate variables based on dose weighted LET (LET_D) to facilitate

implementation into a particle therapy TPS (Treatment Planning System), simply assuming that the particle's energy, and hence also LET, is available in a TPS. Finally, we demonstrate the model's feasibility for proton RBE calculations in a research version of the RayStation TPS (RaySearch Labs, Stockholm).

Methods and materials

Formalism

Based on the linear-quadratic (LQ) formalism we denote the linear and quadric coefficients for a radiation quality Q and tissue T as $\alpha_{Q,T}$ and $\beta_{Q,T}$, where R instead of Q indicates the reference radiation quality, commonly photons. Using the quantities $RBE_{max,T} = \alpha_{Q,T}/\alpha_{R,T}$ and $RBE_{min,T} = \sqrt{\beta_{Q,T}/\beta_{R,T}}$, we follow [9] and express the RBE for a certain radiation quality and tissue at dose D as

$$RBE_{Q,T} = \frac{-\left(\frac{\alpha}{\beta}\right)_{R,T} + \sqrt{\left(\frac{\alpha}{\beta}\right)^2_{R,T} + 4D \cdot RBE_{max,T} \cdot \left(\frac{\alpha}{\beta}\right)_{R,T} + 4D^2 \cdot RBE^2_{min,T}}}{2D}$$

(1)

where $(\alpha/\beta)_{R,T} = \alpha_{R,T}/\beta_{R,T}$. The dependence of $RBE_{min,T}$ on the beam quality has been questioned [10–12], although a recent study suggests a small variation with beam quality [13] for protons. In line with previous studies [14,15] we assume $RBE_{min,T}$ to be unity. Our approach for modelling $RBE_{max,T}$ is inspired by [14,15] where the parameterized $RBE_{max,T}$ for different tissues were inherently scaled with $1/(\alpha/\beta)_{R,T}$. Hence, our ansatz for nanoCluE starts from the identity

$$RBE_{max,T} \equiv \frac{\alpha_{Q,T}}{\alpha_{R,T}} \equiv \frac{1}{(\alpha/\beta)_{R,T}} \frac{\alpha_{Q,T}}{\beta_{R,T}}$$

(2)

in which we treat the ratio $\alpha_{Q,T}/\beta_{R,T}$ to be described with a function $q(n, \mu, b)$

$$\frac{\alpha_{Q,T}}{\beta_{R,T}} = q(n, \mu, b)$$

(3)

where n is a nanodosimetric variable, μ is a microdosimetric variable and $b = (\alpha/\beta)_{R,T}$ serve as a tissue specific "macroscopic" variable. Since we will design n and μ to include most of the variation with Q, the functional dependence needed from $q(n, \mu, b)$ is to be a correction factor, for which we used a second degree polynomial with mixed terms

$$q(n, \mu, b) = q_0 + q_1 n + q_2 \mu + q_3 b + q_4 n\mu + q_5 nb + q_6 \mu b$$
$$+ q_7 n^2 + q_8 \mu^2 + q_9 b^2$$

(4)

where q_0 to q_9 are parameters fitted to experimental LQ data, see sect. 2.2. To determine the nanodosimetric and microdosimetric variables we generated a track structure data base with Geant4-DNA 10.3.3 [16–18], see supplement for details.

Experimental LQ data

We assembled a data base of experimental LQ data by extending our earlier used data [5] with data from published databases [19,20] and elsewhere, see the supplementary material for a full list. For the nanodosimetric part (section2.3) we exclusively used data for the V79 cell line for which ample data are available. Furthermore, we only included cell survival data based on monoenergetic beams, with cells that are not subject to purposely induced mutations and were asynchronous with respect to the cell cycle. For both the microdosimetric part described in section 2.4 and the final parametrization of Eq. (4) described in Section 2.5, we used data for other cell lines than V79, and also non-monoenergetic data provided that the measurements were performed at shallow depths, well upstream of the SOBP. We added the requirement that $\beta_{R,T} > 0$, necessary for the validity of Eq. (4) bearing in mind that the model is intended for tumors and tissues (rather than cell line data) where photon reference values of $(\alpha/\beta)_{R,T}$ are finite. We excluded data for which $(\alpha/\beta)_{R,T} > 20$ considering these unlikely for both cancerous and normal tissues [21,22]. As radiation quality descriptors we used type and LET, with the dose weighted LET_D to estimate LET for non monoenergetic values. For the publications where it was not explicitly provided we used values assigned in reviews [19,20]. For carbon ions, the LET value that included contributions nuclear fragments was chosen if reported.

Nanodosimetry

We used the EDs from the track structure simulations to compute the frequency of cluster order (CO) distributions $f_{CO,Q}$ for different beam qualities using the cluster definition from Bäckström and Villegas et al [5,23]. It gives the frequency, per imparted energy, for clusters of order CO of EDs for which the distance between two adjacent EDs never exceeds a characteristic distance d_C. It follows that the dose fraction deposited by a certain cluster order is proportional to $CO \cdot f_{CO,Q}$, and that the total response can be described as a weighted sum of contributions over the total $f_{CO,Q}$ distribution. Hence, following the formalism of Villegas et al [5], using clusters for the characteristic distance $d_C = 2.5$ nm, we modelled the variable n by fitting weights w_{CO_i} of cluster order bin i for experimental V79 cell line data according to

$$n = \frac{\alpha_{Q,V79}}{\alpha_{R,V79}} \equiv RBE_{max,V79} = \frac{\sum_{i=1}^{k} \left(F_{CO_i,Q} - F_{CO_{i-1},Q}\right) \cdot w_{CO_i}}{\sum_{i=1}^{k} \left(F_{CO_i,R} - F_{CO_{i-1},R}\right) \cdot w_{CO_i}}$$

(5)

where $F_{CO_i,Q} = \sum_{CO=1}^{CO_i} f_{CO,Q} \cdot CO$ are cumulated values to enable binning of cluster orders to limit the overall number of fitted weights to k. For more information, see the supplemental information.

Microdosimetry

At the microdosimetric level, the variable action of different radiation qualities can be attributed to the spread of energy depositions over cell nuclei sized targets. A common descriptor of such distributions, as a microdosimetric analog of LET, is the frequency mean lineal energy $\bar{y}_f$. However, the shape and cavity size for determination of $\bar{y}_f$ varies depending on experimental conditions rather than specified from accepted consensus. Based on extensive Monte Carlo simulations (see supplement) and the work of Villegas et al [8] we have assumed spherical shape and selected a beam quality dependent cavity diameter d_Q such that the mean single track specific energy $\bar{z}_F$ equals the MID (Mean Inactivation Dose), defined as

$$MID(Q) = \int_0^\infty SF(D, Q)dD$$

(6)

where SF is the LQ based survival fraction. The corresponding mean lineal energy denoted as $\bar{y}_{f,MID}$ demonstrate a strong relationship with d_Q almost independent of beam quality suggesting its feasibility as a proxy for microdosimetric characteristics [8]. For use as the variable μ in $q(n, \mu, b)$ of Eq. (4) we used three different base quantities, namely d_Q, $\bar{y}_{f,MID(Q)}$ and LET, the latter because of its widespread usage in RBE models. To compute d_Q and $\bar{y}_{f,MID}$ for a variety of cell lines and beam qualities we used LQ-parameters from the learning set (see the supplementary materials for details). We

here used data for all cell lines in the database, to correct for the bias from the V79 cell lines used in the previous section.

We considered several alternatives for the microdosimetric variable μ in Eq. (4) as to find the one that yielded the best fitting to the learning set data. The considered alternatives were d_Q, $d_Q - d_R$, d_Q/d_R, $\bar{y}_{f,MID(Q)}$, $\bar{y}_{f,MID(Q)} - \bar{y}_{f,MID(R)}$, $\bar{y}_{f,MID(Q)}/\bar{y}_{f,MID(R)}$ and LET. Determination of both d_Q and $\bar{y}_{f,MID(Q)}$ involves data for several cell lines causing numerical variation relative to the corresponding LET value, hence the result was filtered by fitting the coefficients μ_1 and μ_2 to

$$\mu = \mu_1 LET + \mu_2 LET^2 \tag{7}$$

before implementation.

Implementation and testing

Each alternative of μ went through fitting of Eq. (4) with the intent to choose the one yielding the highest adjusted coefficient of determination R^2. Maximizing the adjusted R^2 penalizes the use of additional parameters to avoid overfitting. We tested permutations of Eq. (4) by leaving out terms and scoring the adjusted R^2 for each permutation, in a manner such that b appeared in at least one term for each test. To account for the published uncertainties of the LQ-parameters, a bootstrapping technique was used for which each (α, β) entry was represented by five sampled entries (increasing the number did not change the results much) from normal distributions with standard deviations as given in the references for each data entry. To deal with the paucity of data for low LET, we used a weight of 3 (relative 1 for the rest) for data points with an LET $\leqslant 3$ keV/μm to ensure RBE values of around 1 in the plateau region. The fits were done versus the same learning set as for determination of $\bar{y}_{f,MID(Q)}$ and d_Q. To simplify TPS implementations, both n and the finally selected variable for μ were pre-computed as a function of LET and particle type. Given the relatively smooth variation of n with LET, it was interpolated between the pre-calculated values, while μ was parameterized according to Eq. (7).

For testing we compared results from our model with previously published models; for protons we used the McNamara model [24] and the Tilly-Wedenberg model [14,15]. For carbon ions, we used the RMF model [25] and an in-house implementation of the mMKM model [4]. All models were implemented in a research version (9A-IonPG 8.99.30) of the RayStation TPS. For the RMF model we assumed a fixed cell nucleus diameter of 4 μm [26] whilst allowing $\alpha_{R,T}$ and $\beta_{R,T}$ to vary [27]. For the mMKM model we used fixed values of cell nucleus radius R_n = 3.9 μm and domain radius r_d = 0.32 μm [4] and $\alpha_{R,T}$ and $\beta_{R,T}$ could varied [28]. The quantities used for comparison were $RBE_{max,T}$ and the RBE for a dose of 2 Gy, $RBE_{Q,T,2Gy}$. As comparison metric we used the root mean square error (RMSE) summed over the available data base. To reduce bias for nanoCluE we used the leave one out procedure in which the model was refitted without the test data point.

For test points of $RBE_{Q,T,2Gy}$ where experimental β_Q were not provided we assumed $RBE_{min,T}$ = 1. i.e. for the nanoCluE, mMKM and Tilly-Wedenberg models we assumed in all cases $RBE_{min,T}$ = 1. The McNamara and RMF models includes a tissue and beam quality dependent RBE_{min} that was used. At the voxel level for TPS applications, we calculated dose weighted values of RBE_{max} for the spectrum of particles imparting dose to the voxel before entering the value into the final, voxel level calculations of RBE. We only considered primary protons when calculating LET in RayStation in line with earlier findings when applying nanoCluE for protons [29].

Results

The form of the function $q(n,\mu,b)$ of Eq. (4) that yielded the highest adjusted R^2 = 0.874 was with μ equal to d_Q, and included all but the μ^2-term. With coefficient values this is

$$q(n,\mu,b) = 0.170 - 0.944n + 5.23\mu + 0.519b - 0.476n\mu$$
$$+ 0.706nb - 0.233\mu b + 0.181n^2 - 0.0117b^2 \tag{8}$$

with q expressed in Gy^{-1}, with n dimensionless, μ in μm and b in Gy. Excluding μ, i.e. $q = q(n,b)$, the highest adjusted R^2 = 0.865. Excluding instead n, i.e. $q = q(\mu,b)$, the highest adjusted R^2 = 0.782.

The final fitted forms of Eq. (7) for protons and carbon ions were

$$\mu_{H^+} = 0.129 LET - 2.12 \cdot 10^{-3} LET^2$$
$$\mu_{C12^{6+}} = 0.0259 LET - 2.65 \cdot 10^{-5} LET^2 \tag{9}$$

with μ in μm and LET in keV/μm.

The results of nanoCluE RBE_{max} for carbon ions and protons compared to experimental values are shown in Fig. 1, separately for different classes of α/β values of the reference radiation. Residuals as function of LET are shown in Fig. 2 together with RMSE values for nanoCluE, for carbon ions the mMKM and the RMF models, and for protons the Tilly-Wedenberg and the McNamara models. For carbon ions the RMSE value for nanoCluE is about 43 % lower than that for the mMKM model, and less than half than that of the RMF model (nanoCluE 2.26, mMKM 3.24, RMF 5.24) while for protons nanoCluE demonstrate similar results as the other models (nanoCluE 1.57, Tilly-Wedenberg 1.31, McNamara 1.30).

Comparing the models with experimental RBE at 2 Gy yielded for carbon ions better results for all models (nanoCluE 0.45, mMKM 0.63, RMF 3.36) and so also for protons (nanoCluE 0.62, Tilly-Wedenberg 0.52, McNamara 0.55).

For protons the TPS implementation is demonstrated in Fig. 3 for $(\alpha/\beta)_{R,T}$ = 3 for a proton SOBP with a modulation depth of 10 cm and total range of 20 cm in a water phantom. Results are shown for the nanoCluE, Tilly-Wedenberg and McNamara models and for a constant RBE = 1.1. For the nanoCluE and Tilly-Wedenberg models $RBE_{min,T}$ = 1 was assumed, whilst for the McNamara model a LET-dependent value for $RBE_{min,T}$ was used. All models present the characteristic increase in RBE towards the end of the spread out Bragg peak but with different magnitudes. At 1 cm depth, the nanoCluE predicted a 7 % lower RBE weighted dose than if using RBE = 1.1, as compared to 4 % and 1 % for Tilly-Wedenberg and McNamara, respectively. At 20 cm depth at the end of the SOBP, nanoCluE predicts an 11 % higher RBE weighted dose than if using RBE = 1.1, as compared to 14 % for both the Tilly-Wedenberg and McNamara models. It is likely that optimizing treatment plans using an RBE model such as nanoCluE will
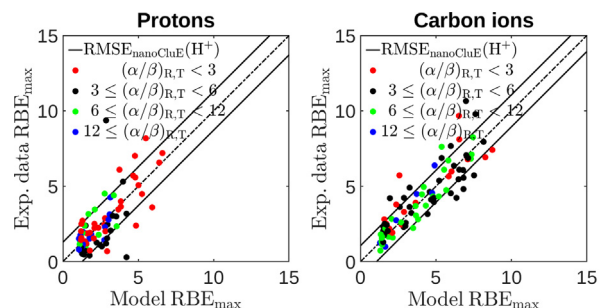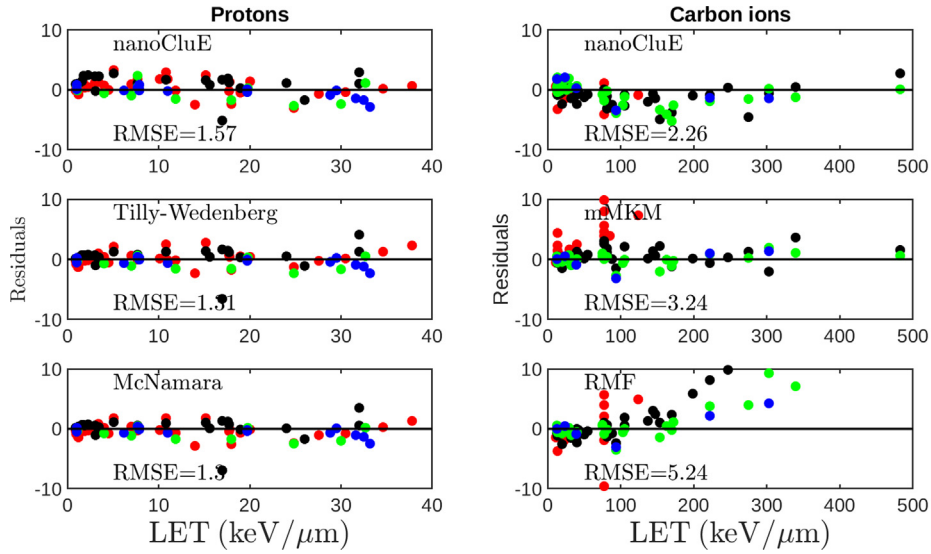

Fig. 1. *The experimental RBE_{max} plotted versus RBE_{max} as given by nanoCluE, i.e. Eq. (3) with $q(n,\mu,b)$ as given by Eq. (8) for protons (left) and carbon ions (right). Discs represent experimental data. The dashed-dotted line represent an ideal model. The solid curves represent the RMSE of nanoCluE.*

Fig. 2. Residuals vs LET for the considered RBE models for protons and carbon ions. Data points are color-coded as in Fig. 1.The nanoCluE residuals were obtained by the leave one out procedure.
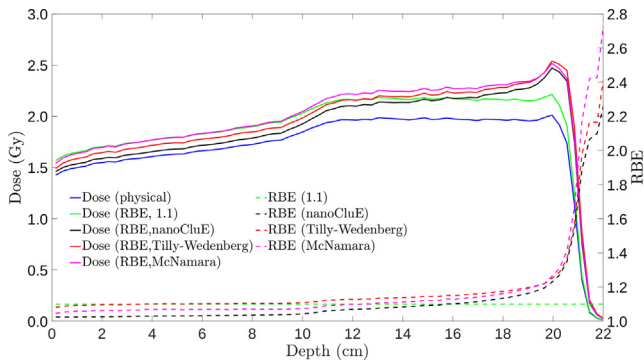
Fig. 3. A proton SOBP along with the variable RBE as predicted by nanoCluE, Tilly-Wedenberg and McNamara models (solid curves) together with constant RBE. Also shown are the RBE curves (dashed curves) for the models.

reduce the RBE modelled dose burden to the OARs (organs at risk). Albeit somewhat anecdotal, this is demonstrated in Fig. 4 for a H&N patient prescribed a mean dose of 70 Gy with optimization goals of $D_{98\%} > 66.5$ Gy and $D_{2\%} < 73.5$ Gy planned with either RBE 1.1 or nanoCluE modelled RBE. After robustness evaluation using 28 different scenarios of isotropic 4 mm isocenter displacements
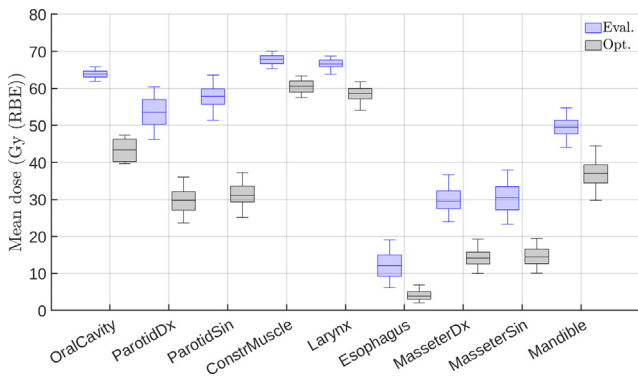

Fig. 4. Result of robustness evaluation expressed as mean nanoCluE RBE weighted dose for 28 scenarios to organs at risk for a head&neck patient prescribed a mean target dose of 70 Gy. Blue boxes show results for plans optimized with RBE = 1.1, while black boxes show data for plans optimized with nanoCluE.

and 3.5 % Hounsfield value uncertainty, the figure shows the resulting distributions of mean RBE modelled doses for selected OARs. For the target, the median of the evaluated nanoCluE RBE $D_{98\%}$ dose is reduced from 75.1 Gy for RBE 1.1 planning to 67.4 Gy with nanoCluE planning.

The quantity resulting from the nanodosimetric modelling, i.e. $n = \alpha_{Q,V79}/\alpha_{R,V79}$ is shown for protons and carbon ions in Fig. 5 as a function of LET. The cumulative functions $F_{CO_i,Q}$ and the resulting w_{CO_i} used for its determination are presented in the supplement. For protons, n increases with increasing LET from unity, indicating a similar biological damage efficacy for ^{60}Co as for higher energy protons. For carbon ions, n increases with LET until it reaches a peak at about 170 keV/μm. At higher values of LET, n decreases due to overkill [30], in accordance with experimental data for several particle types [31]. The resulting microdosimetric quantity d_Q selected as μ is also shown in Fig. 5 as function of LET.

Discussion

In this work we present the nanoCluE RBE model which incorporates nano- and microdosimetric variables together with a tissue
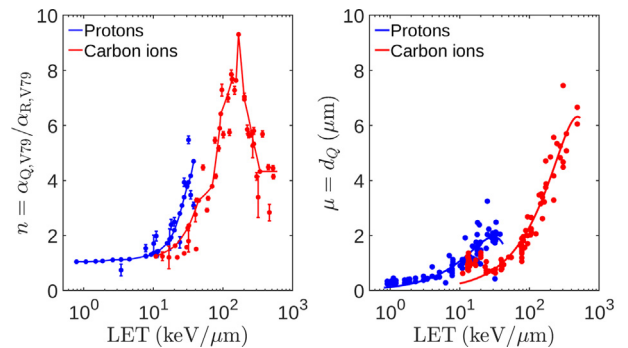
Fig. 5. (left) The quantity $\alpha_{Q,V79}/\alpha_{R,V79}$ resulting from the nanodosimetric modelling (and used for n in Eqs. (3) and (4)) shown for protons (blue) and carbon ions (red). The experimental data are shown with error bars, while the modelled results from Eq. (9) are shown as dots connected by lines. The dots are located at the LET values for which Monte Carlo track structure simulations were done. (right) The quantity d_Q resulting from the microdosimetric modelling (and used as μ in Eqs. (3) and (4)) shown for protons (blue) and carbon ions (red). The data points stems from the experimental LQ-parameters that d_Q depends on. The solid lines represents the particle specific fits of Eq. (9) for protons (blue) and carbon ions (red).

specific factor. It has been developed to predict the RBE for proton and carbon ions over a wide LET range and tissues/tumors characterized by different values of $(\alpha/\beta)_{R,T}$. We have also demonstrated its simplicity for its implementation into a TPS, albeit only for protons, through use of LET as the independent variable.

For carbon ions nanoCluE proved superior among the tested models. However, the usage of fixed cell nuclei diameters and domain sizes for RMF and mMKM may have limited their accuracy, although the latter is used clinically with fixed values [4]. Specific values for these parameters are not readily available for all tissue/-tumor types, and thus we followed the example of earlier published work [27] in using fixed values for these parameters, but allowing $(\alpha/\beta)_{R,T}$ to vary. A major limitation for all RBE-models is the lack of *in vivo* data necessitating the use of *in vitro* radiobiological data as learning data. The large variation in methodology of the published data increases the uncertainties of the available LQ-parameters [19] in addition to scarcity of data for less common radiation modalities. The uncertainties propagate into model uncertainty. For protons all the tested models yielded similar results suggesting that the precision limit a phenomenological model can reach is achieved and thus limited by the uncertainty in experimental data. Not surprisingly, all proton models yield lower RMSE than simply using the constant 1.1 factor. Clinically, even small variations in RBE may become important when the target is in close proximity to an OAR, especially if the OAR has a low $(\alpha/\beta)_{R,T}$ and is a serial organ [32].

Given the datasets of LQ-parameters used in our work no strong correlation between the introduced quantities and RBE_{min} could be found. We therefore resorted to assuming that $RBE_{min} = 1$ independent of beam quality. One study based on published experimental data found a weak correlation between $\beta_{Q,T}$ and LET for low doses and low values of $(\alpha/\beta)_{R,T}$ [13], which easily could be applied due to the overall LQ-formalism used in nanoCluE.

Handling of heavy secondary particles with high RBE could impose problems. However, in an earlier study [29] we showed that for protons it is consistent to assume that experimental LQ-parameters include the effects of heavy secondaries, and therefore not needed be explicitly considered for treatment planning applications. Another problem inherent to all RBE models is the large intra-voxel variance in the deposited dose toward the end of the particle range. This is caused by a high probability that particles stop within the voxel, as well as reductions in the particle fluence and range of the secondaries. These factors may lead to an increased likelihood of tumor cells in part of the voxel avoiding all hits causing the tumor control probability at the voxel to approach zero despite high RBE and finite dose. We know of no solution to accurately calculate a meaningful RBE for these circumstances.

In this work we addressed only protons and carbon ions. The framework for the nano- and microdosimetric variables is particle agnostic although tested only for those two species. Excluding the μ-component in q caused a smaller difference to the adjusted R^2-value than excluding the n-component. It indicates that the nano-metric scale phenomena might be more important than the microdosimetric parts, with the latter effectively serving as a correction. Further work is needed to investigate the applicability of those features as building blocks for RBE-models applied to helium, boron or other ions.

Conclusion

In this work we have presented nanoCluE, an *RBE* model that combines nanodosimetric and microdosimetric quantities with the macroscopic tissue dependent α/β-value for photons. All resulting beam quality dependent parameters are for protons and

carbon ions expressed as function of LET to facilitate implementation into a TPS for calculations in a voxelized anatomy. For carbon ions, nanoCluE showed better RMSE values versus experimental data than the mMKM and the RMF models, suggestive of nano-CluE's potential to model carbon ion RBE, motivating further exploration of its use. Compared to the Tilly-Wedenberg and McNamara models for protons, the nanoCluE showed similar RMSE when comparing its prediction of RBE_{max} to published experimental LQ-parameters. For RBE evaluated at 2 Gy, all variable phenomenological proton RBE models gave a smaller standard deviation than using the fixed 1.1, with nanoCluE having the smallest.

Conflict of Interest Statement

Erik Traneus is an employee of RaySearch Laboratories. Nina Tilly is an employee of Elekta Instrument.

Appendix A. Supplementary material

Supplementary data to this article can be found online at https://doi.org/10.1016/j.radonc.2023.109539.

References

[1] ICRU. Report 78: Prescribing, recording and reportin proton-beam therapy. J ICRU 2007;7.
[2] Scholz M, Kraft G. Track structure and the calculation of biological effects of heavy charged particles. Adv Space Res 1995;18:5–14.
[3] Hawkins RB. A microsdosimetric-kinetic model for the effect of non-poisson distribution of lethal lesions on the variation of RBE with LET. Radiat Res 2003;160:61–9.
[4] Inaniwa T, Furukawa T, Kase Y, Matsufuji N, Toshito T, Matsumoto Y, et al. Treatment planning for a scanned carbon beam with a modified microdosimetric kinetic model. Phys Med Biol 2010;55:6721–37.
[5] Villegas F, Bäckström G, Tilly N, Ahnesjö A. Energy deposition clustering as a functional radiation quality descriptor for modeling relative biological effectiveness. Med Phys 2016;43:6322–35.
[6] Goodhead DT. Energy deposition sotchastics and track structure: what about the target? Radiat Prot Dosim 2006;122:3–15.
[7] Kellerer AM, Chmelevsky D. Concepts of Microdosimetry II. Probability distributions of the microdosimetry variables. Radiation Environ Biophys 1975;12:205–16.
[8] Villegas F, Tilly N, Ahnesjö A. Target size variation in microdosimetric distributions and its impact on the linear quadradic parameterization of cell survival. Radiat Res 2018;190:504–12.
[9] Carabe-Fernandez A, Dale RG, Jones B. The incorporation of the oncept of minimum RBE (RBEmin) into the linear-quadratic model and the potential for improved radiobiological analysis of high-LET treatments. Int J Radiat Biol 2007;83:27–39.
[10] Ando K, Goodhead DT. Depedence and indepdence of survival parameters on linear energy transfer in cells and tissues. J Radiat Res 2016;57:596–606.
[11] Hawkins RB. A statistical theory of cell killing by radiation of varying linear energy transfer. Radiat Res 1994;140:366–74.
[12] Kellerer AM, Rossi HH. The theory of dual radiation action. Curr Topics Radiation Res 1974;8:85–158.
[13] Rørvik E, Thörnqvist S, Ytre-Hauge KS. The experimental dose ranges influence the LETd dependency of the proton minimum RBE (RBEmin). Phys Med Biol 2019;64:1–9.
[14] Tilly N, Johansson J, Isacsson U, Medin J, Blomquist E, Grusell E, et al. The influence of RBE variations in a clinical proton treatment plan for a hypopharynx cancer. Phys Med Biol 2005;50:2765–77.
[15] Wedenberg M, Lind BK, Hårdemark B. A model for the relative biological effectiveness of protons: the tissue specific parameter α/β of photons is a predictor for the sensitivity to LET changes. Acta Oncol 2013;52:580–8.

[16] Incerti S, Ivanchenko A, Karamitros M, Mantero A, Moretto P, Tran HN, et al. Comparison of Geant4 very low energy cross section models with experimental data in water. Med Phys 2010;37:4962–5708.

[17] Bernal MA, Bordage MC, Brown JMC, Davidková M, Delage E, Bitar ZE, et al. Track structure modeling in liquid water: A review of the Geant4-DNA very low energy extension of the Geant4 Monte Carlo simulation toolkit. Phys Med 2015;31:861–74.

[18] Incerti S, Kyriakou I, Bernal MA, Bordage MC, Francis Z, Guatelli S, et al. Geant4-DNA example applications for track structure simulations in liquid water: a report from the Geant4-DNA project. Med Phys 2018;45:e722–39.

[19] Paganetti H. Relative biological effectiveness for proton beam therapy: variations as a function of biological endpoint, dose and linear energy transfer. Phys Med Biol 2014;59:R419–72.

[20] Friedrich T, Scholz U, Elsässer T, Durante M, Scholz M. Systematic analysis of RBE and related quantities using a database of cell survival experimenets with ion beam irradiation. J Radiat Res 2013;54:494–514.

[21] Thames HD, Bentzen SM, Turesson I, Overgaard M, Bogaert WV. Time-dose factors in radiotherapy: a review of human data. Radiother Oncol 1990;19:219–35.

[22] Van Leeuwen CM, Oei AL, Crezee J, Bel A, Franken NAP, Stalpers LJ, et al. The alfa and beta of tumors: a review of parameters of the linear-quadratic model, derived from clinical radiotherapy studies. Radiat Oncol 2018;13.

[23] Bäckström G, Galassi ME, Tilly N, Ahnesjö A, Fernández-Varea JM. Track structure of protons and other light ions in liquid water: applications of the LIonTrack code at the nanometer scale. Med Phys 2013;40:064101.

[24] McNamara AL, Schuemann J, Paganetti H. A phenomenological relative biological effectiveness (RBE) model for proton therapy based on all published in vitro cell survival data. Phys Med Biol 2015;7:8399–416.

[25] Carlson DJ, Stewart RD, Semenenko VA, Sandison GA. Combined use of Monte Carlo DNA damage simulations and deterministic repair models to examine putative mechanisms of cell killing. Radiat Res 2008;169:447–59.

[26] Stewart RD, Carlson DJ, Butkus MP, Hawkins R, Friedrich T, Scholz M. A comparison of mechanism-inspired models for particle relative biological effectiveness (RBE). Med Phys 2018;45.

[27] Freese MC, Yu VK, Stewart RD, Carlson DJ. A mechanism-based approach to predict the relative biological effectiveness of protons and carbon ions in radiation therapy. Int J Radiat Oncol Biol Phys 2012;83:442–50.

[28] Mein S, Klein C, Kopp B, Magro G, Harrabi S, Karger CP, et al. Assessment of RBE-Weighted dose models for carbon ion therapy toward modernization of clinical practice at HIT. In vitro, in vivo, and in patients. Int J Radiat Oncol Biol Phys 2020;108:779–91.

[29] Almhagen E, Traneus E, Ahnesjö A. Handling of beam spectra in training and application of a proton RBE model. Phys Med Biol 2021;66.

[30] Jones B, Hill MA. Physical characteristics at the turnover-points of relative biological effect (RBE) with linear energy transfer (LET). Phys Med Biol 2019;64.

[31] Sørensen BS, Overgaard J, Bassler N. In vitro RBE-LET dependence for multiple particle types. Acta Oncol 2011;50:757–62.

[32] Paganetti H, Blakely E, Carabe-Fernandez A, Carlson DJ, Das IJ, Dong L, et al. Report of the AAPM TG-256 on the relative biological effectiveness of proton beams in radiation therapy. Med Phys 2019;46:e53–78.